

ANGARFITE, $\text{NaFe}^{3+}_5(\text{PO}_4)_4(\text{OH})_4 \cdot 4\text{H}_2\text{O}$, A NEW MINERAL SPECIES FROM THE ANGARF-SUD PEGMATITE, MOROCCO: DESCRIPTION AND CRYSTAL STRUCTURE

ANTHONY R. KAMPF[§] AND STUART J. MILLS[¶]

*Mineral Sciences Department, Natural History Museum of Los Angeles County, 900 Exposition Boulevard,
 Los Angeles, California 90007, U.S.A.*

ROBERT M. HOUSLEY

Division of Geological and Planetary Sciences, California Institute of Technology, Pasadena, California 91125, U.S.A.

GEORGES FAVREAU

421, avenue Jean Monnet, F-13090 Aix-en-Provence, France

JEAN-CLAUDE BOULLIARD AND VINCENT BOURGOIN

*Association Jean Wyart, Collection des Minéraux de Jussieu, IMPMC, Université Pierre-et-Marie-Curie,
 case courrier 73, 4, place Jussieu, F-75252 Paris Cedex 05, France*

ABSTRACT

Angarfite, ideally $\text{NaFe}^{3+}_5(\text{PO}_4)_4(\text{OH})_4 \cdot 4\text{H}_2\text{O}$, is a new mineral from the Angarf-Sud pegmatite, Tazenakht, Ouarzazate Province, Souss-Massa-Draâ region, Morocco. The mineral occurs on etched surfaces of triphylite in association with lipscombe-barboselite, jahnsite-(NaFeMg) and bederite. It is interpreted as having resulted from the reaction of Na-bearing hydrothermal solutions with primary triphylite. The crystals are orange-brown to red-brown needles and prisms, elongate on [001], with poorly formed chisel-like terminations. The mineral is transparent and has a pale brown streak, a vitreous luster, a Mohs hardness of approximately 2½, a splintery fracture and one poorly developed cleavage on {010}. It is brittle, but thin needles are slightly flexible. The measured and calculated densities are 2.76(3) and 2.771 g/cm³, respectively. It is optically biaxial (+), $\alpha = 1.688(1)$, $\beta = 1.696(1)$, $\gamma = 1.708(2)$ (white light); $2V_{\text{meas}} = 80(3)^\circ$; $2V_{\text{calc}} = 79^\circ$; strong r > v dispersion; optical orientation: $X = \mathbf{b}$, $Y = \mathbf{c}$, $Z = \mathbf{a}$; pleochroism: X is tan, Y, medium red-brown, and Z, dark red-brown, with $X < Y < Z$. The average results of five electron-microprobe analyses gave Na_2O 2.69, MgO 4.76, Mn_2O_3 1.79, Fe_2O_3 37.36, P_2O_5 34.68, H_2O 14.63 (from structure refinement), total 95.91 wt%. The empirical formula, based on 24 O atoms, is $\text{Na}_{0.71}(\text{Fe}^{3+})_{3.83}\text{Mg}_{0.97}\text{Mn}_{0.19}\Sigma 4.99(\text{P}_{1.00}\text{O}_4)_4(\text{OH})_{2.71}(\text{H}_2\text{O})_{1.29} \cdot 4\text{H}_2\text{O}$. Angarfite is orthorhombic, $C222_1$, $a = 12.7997(3)$, $b = 17.9081(4)$, $c = 8.2112(6)$ Å, $V = 1882.16(15)$ Å³ and $Z = 4$. The eight strongest lines in the X-ray powder-diffraction pattern [d_{obs} in Å(I)(hkl)] are: 10.463(43)(110), 9.016(100)(020), 6.459(42)(111), 3.731(27)(022), 3.355(51)(241), 3.026(29)(042), 1.926(33)(462, 263), 1.463(36)(822, 663, 4102, 2103). The crystal structure ($R_1 = 3.02\%$ for 2074 reflections, $F_o > 4\sigma F$) contains zig-zag chains of edge-sharing Fe^{3+}O_6 octahedra along \mathbf{c} , which are linked into sheets parallel to {010} by sharing corners with octahedra in adjacent chains and by sharing corners with peripheral PO_4 tetrahedra. Insular octahedra between the sheets share two sets of *cis* corners with tetrahedra in adjacent sheets, thereby linking the sheets into a framework. Channels in the framework parallel to \mathbf{c} contain a partially occupied Na site and a disordered H_2O site. Identical sheets of octahedra and tetrahedra are found in the structures of bakhchisaraitsevite and mejillonesite.

Keywords: angarfite, new mineral species, phosphate, crystal structure, bakhchisaraitsevite, mejillonesite, Angarf-Sud pegmatite, Morocco.

[§] E-mail address: akampf@nhm.org

[¶] Current address: Geosciences, Museum Victoria, GPO Box 666, Melbourne 3001, Victoria, Australia.

SOMMAIRE

L'angarfite, idéalement $\text{NaFe}^{3+}_5(\text{PO}_4)_4(\text{OH})_4 \bullet 4\text{H}_2\text{O}$, est une nouvelle espèce minérale provenant de la pegmatite d'Angarf-Sud, Tazenakht, province d'Ouarzazate, région du Souss-Massa-Draâ, au Maroc. Le minéral se présente sur des surfaces corrodées de triphylite en association avec lipscombeite-barbosalite, jahnsite-(NaFeMg) et bederite. On interprète le minéral comme un produit de la réaction de solutions hydrothermales contenant du sodium et de la triphylite primaire. Les cristaux sont des baguettes et des prismes brun-orangé à brun-rouge, allongés selon [001], avec des terminaisons mal formées en forme de burin. Le minéral est transparent avec un trait brun clair, éclat vitreux, dureté de Mohs approximative de 2½, cassure esquilleuse et un clivage très imparfait selon {010}. Il est cassant, mais les aiguilles les plus fines sont légèrement flexibles. Les densités mesurée et calculée sont respectivement de 2,76(3) et 2,771 g/cm³. Le minéral est optiquement biaxe (+), α 1,688(1), β 1,696(1), γ 1,708(2) (lumière blanche); $2V_{\text{mes}} = 80(3)^\circ$; $2V_{\text{calc}} = 79^\circ$; dispersion $r > v$ forte; orientation optique: $X = \mathbf{b}$, $Y = \mathbf{c}$, $Z = \mathbf{a}$; pléochroïsme: X est brun-roux, Y , brun-rouge moyen, et Z , brun-rouge sombre, avec $X < Y < Z$. Les analyses à la microsonde électronique (moyenne de cinq mesures) ont donné: Na_2O 2,69, MgO 4,76, Mn_2O_3 1,79, Fe_2O_3 37,36, P_2O_5 34,68, H_2O 14,63 (déduit de la structure), total de 95,91% en masse. La formule empirique, fondée sur 24 atomes d'oxygène, est $\text{Na}_{0.71}(\text{Fe}^{3+}_{3.83}\text{Mg}_{0.97}\text{Mn}^{3+}_{0.19})_{24.99}(\text{P}_{1.00}\text{O}_4)_4(\text{OH})_{2.71}(\text{H}_2\text{O})_{1.29} \bullet 4\text{H}_2\text{O}$. L'angarfite est orthorhombique, $C222_1$, a 12,7997(3), b 17,9081(4), c 8,2112(6) Å, V 1882,16(15) Å³ et $Z = 4$. Les huit raies les plus intenses dans le diagramme de diffraction X prélevé sur poudre [d_{obs} en Å(I)/(hkl)] sont: 10,463(43) (110), 9,016(100)(020), 6,459(42)(111), 3,7311(27)(022), 3,3550(51)(241), 3,0261(29)(042), 1,9259(33)(462, 263), 1,4626(36) (822, 663, 4102, 2103). La structure cristalline ($R_1 = 3.02\%$ pour 2074 $F_o > 4\sigma F$) comporte des chaînes en zig-zag d'octaèdres Fe^{3+}O_6 partageant des arêtes le long de \mathbf{c} , reliées en feuillets parallèles à {010} par le partage de sommets avec des octaèdres des chaînes adjacentes et avec des tétraèdres PO_4 périphériques. Les octaèdres insulaires entre les feuillets partagent deux ensembles de sommets *cis* avec des tétraèdres des feuillets adjacents, reliant ainsi les feuillets au sein d'un réseau. Les canaux du réseau parallèles à \mathbf{c} contiennent un site Na partiellement occupé et un site H_2O désordonné. Des feuillets identiques d'octaèdres et tétraèdres sont rencontrés dans les structures de la bakhchisaraïtsévite et de la mejillonesite.

Mots-clés: angarfite, nouvelle espèce minérale, phosphate, structure cristalline, bakhchisaraïtsévite, mejillonesite, pegmatite d'Angarf-Sud, Maroc.

INTRODUCTION

The Angarf-Sud (or Angarf-South) granitic pegmatite is the best documented and most extensively researched occurrence of pegmatite phosphates in North Africa (Fransolet 1975, 1987, Fransolet *et al.* 1985); it is the type locality of mélonjosephite (Fransolet 1973, Kampf & Moore 1977). Beryl was discovered at Angarf-Sud in 1946, and mining, mostly in the early 1950s, yielded a total of about 450 tonnes of beryl (Jouravsky & Destombes 1961). The suite of about 30 phosphates known from the pegmatite is found in nodules that occur in the microcline-rich intermediate zone (see below). Because the nodules were not of economic value, they were discarded during the mining of the intermediate zone for beryl and mica. Although phosphate nodules can still rarely be observed in place in the intermediate zone, most of those studied have been recovered from the dumps. The new mineral angarfite, reported herein, was found during recent systematic collecting of phosphate nodules in the dumps. Only one nodule containing angarfite was found.

The new mineral and name have been approved by the Commission on New Minerals, Nomenclature and Classification of the International Mineralogical Association (IMA 2010-082). The two cotype specimens used in the description of the mineral are housed in the mineral collection of the Natural History Museum of Los Angeles County under catalogue numbers 63428 and 63429.

OCCURRENCE

The Angarf-Sud pegmatite (Fig. 1) is located on the Zenaga (or Znaga) plain in the Anti-Atlas Mountains of southern Morocco, near the town of Tazenakht, Ouarzazate Province, Souss-Massa-Draâ Region, Morocco (43°39'30"N, 2°29'58"E). The Tazenakht leucocratic granite outcrops sporadically throughout the Zenaga Plain, from the north near Tazenakht, to the south where it forms the Adghagh massif. Thick veins of pegmatitic granite and pegmatites, including Angarf-Sud, emanate from the northeastern side of the massif and are dated at up to 2,035 million years old (Thomas *et al.* 2002).

As noted by Fransolet *et al.* (1985), the Angarf-Sud pegmatite, measuring 100 × 25 m, is a subelliptical, zoned body oriented north-northeast. The pegmatite core is a mass of quartz 15 m thick, which is surrounded by an intermediate zone containing giant (3 to 4 m³) microcline crystals and quartz. The intermediate zone hosted the mica and beryl, for which the pegmatite was mined. Beyond the intermediate zone is a one-meter thick margin, rich in muscovite and quartz. The surrounding subvertical mica schists are locally enriched in black tourmaline. The main masses of phosphate occur as nodules of altered euhedral-to-subhedral crystals of triphylite in the intermediate zone at its contact with the quartz core (Fig. 2). They were mainly located on the south side of the quarry.

The nodules are generally 10 to 20 cm in diameter, but in exceptional cases, they attain 50 cm. According to Fransolet (1987), and as observed in our studies as well, the nodules commonly show the following zonal

tion from core to rim: 1) A core of compact Mg-rich triphylite of grayish color with a greenish to brownish tint. Angarfite was found in such a material. 2) A layer of green to dark green phosphates close in composition to Fe- and Ca-bearing alluaudite, rooted in the triphylite, in some cases deeply. 3) A rather regular layer of microcrystalline fluorapatite with a shell-like fracture, of reddish to purplish color (generally tinted by hematite) and clearly separated from the previous layer. 4) A fourth layer, more difficult to observe, with muscovite, scorzalite, quartz and pyrite.

The phosphates are attributed to three genetic processes, each characterized by specific species: primary crystallization in the pegmatite, hydrothermal alteration and surface weathering.

Angarfite was found in a complete nodule (15 cm across) exhibiting a crust of purplish gray fluorapatite around a core of triphylite transected by narrow veins. The angarfite needles occur in these veins, on etched surfaces of triphylite (not greater than 5 mm² in area) in association with lipscombe–barboselite, jahnsite-(NaFeMg) and bederite. The only other reported occurrence of jahnsite-(NaFeMg) is the Tip Top pegmatite, Custer County, South Dakota, USA (Kampf *et al.* 2008) and the only other occurrence of bederite is the El Peñón pegmatite, Nevados de Palermo, Salta, Argentina (Galliski *et al.* 1999). Angarfite has apparently resulted from the reaction of Na-bearing hydrothermal solutions with primary triphylite.

PHYSICAL AND OPTICAL PROPERTIES

Angarfite most commonly occurs as orange-brown to red-brown needle-like crystals up to 2 mm in length and 20 µm in diameter, but crystals are usually much smaller (Fig. 3). Much less commonly, it occurs as prismatic crystals up to 0.25 mm in length and 50 µm in diameter. The prism forms include {110}, {100} and {010}; the faces are generally poorly formed and difficult to measure, with chisel-like terminations that are best represented by the {601} form (Figs. 4, 5). Diameter-to-length aspect ratios vary from about 1:5 (prisms) to 1:100 (needles). No twinning was observed.

The mineral is transparent and has a vitreous luster. It has a pale brown streak and a Mohs hardness of approximately 2½. It is brittle, but thin needles are slightly flexible. The fracture is splintery, and there is one poorly developed cleavage on {010}. The density measured by sink–float in an aqueous solution of sodium polytungstate is 2.76(3) g/cm³. The density calculated on the basis of the empirical formula and the single-crystal cell is 2.771 g/cm³.

The mineral is optically biaxial (+), with the following optical constants measured in white light: α 1.688(1), β 1.696(1) and γ 1.708(2). The 2V determined by direct conoscopic measurements using a spindle stage is 80(3)°; the calculated 2V is 79°. Dispersion is

strong, $r > v$. The optical orientation is $X = \mathbf{b}$, $Y = \mathbf{c}$, $Z = \mathbf{a}$. The mineral is pleochroic, with X tan, Y medium red-brown, and Z dark red-brown, with absorption: $X < Y < Z$.

CHEMICAL COMPOSITION

Chemical analyses (5) were carried out using a JEOL 8200 electron microprobe at the Division of Geological and Planetary Sciences, California Institute of Technology (WDS mode, 15 kV, 10 nA, beam diameter 10 µm). Results of quantitative elemental microanalyses were processed with the CITZAF correction procedure (Armstrong 1995). The small amount of material available did not allow for the direct determination of H₂O, so it was calculated by stoichiometry from the results of the crystal-structure analysis. No other elements were detected. The reason for the low analytical total is not clear, but is likely related to measurement of a small amount of epoxy due to the thinness of the angarfite fibers analyzed. Analytical data are given in Table 1.

The empirical formula, based on 24 O atoms, is $\text{Na}_{0.71}(\text{Fe}^{3+})_{3.83}\text{Mg}_{0.97}\text{Mn}^{3+}_{0.19})\Sigma 4.99(\text{P}_{1.00}\text{O}_4)_4(\text{OH})_{2.71}(\text{H}_2\text{O})_{1.29}\bullet 4\text{H}_2\text{O}$. The ideal formula is $\text{NaFe}^{3+}_{5}(\text{PO}_4)_4(\text{OH})_4\bullet 4\text{H}_2\text{O}$, which requires Na₂O 3.77, Fe₂O₃ 48.56, P₂O₅ 34.53, H₂O 13.15, total 100.00%. Angarfite is insoluble in concentrated HCl.

The Gladstone–Dale compatibility index, $1 - (\text{K}_p/\text{K}_c)$, as defined by Mandarino (1981), provides a measure of the consistency among the average index of refraction, calculated density and chemical composition. For angarfite, the compatibility index is 0.038 (excellent) on the basis of the empirical formula.

X-RAY CRYSTALLOGRAPHY AND STRUCTURE DETERMINATION

Both powder and single-crystal X-ray studies were carried out using a Rigaku R-Axis Rapid II curved imaging plate microdiffractometer, with monochromatized MoKα radiation. For the powder-diffraction study, observed values of d and intensities were derived by profile fitting using the JADE 9.1 software (Materials Data, Inc.). The powder data presented in Table 2 show good agreement with the pattern calculated from the structure determination. Unit-cell parameters refined from the powder data using JADE 9.1 with whole-pattern fitting are: a 12.788(3), b 17.894(4), c 8.195(2) Å and V 1875.1(8) Å³.

The Rigaku CRYSTALCLEAR software package was used to process the structure data, including the application of a numerical (shape-based) absorption correction. The structure was solved by direct methods using SIR2004 (Burla *et al.* 2005); the location of all non-hydrogen atoms in the framework was straightforward. We used SHELXL-97 (Sheldrick 2008) for the refinement of the structure. A difference-Fourier synthesis



FIG. 1. A portion of the quarry exploiting the Angarf-Sud pegmatite viewed looking south, with Djebel Adghagh in the distance. Field of view (FOV) in foreground is about 8 m across.

allowed us to locate partially occupied Na and H₂O sites in the channels of the structure, as well as H atom sites associated with framework OH and H₂O sites. The H atoms corresponding to the disordered H₂O sites in the channel, OW2A and OW2B, could not be located; because of the consequent uncertainty in assigning hydrogen bonds from the channel H₂O molecule, no corresponding bond-valence contributions are included in the bond-valence analysis. It is likely that the low bond-valence sums for some of the other O atoms are at least partially compensated by hydrogen bonds from the channel H₂O molecule.

TABLE 1. CHEMICAL ANALYTICAL DATA FOR ANGARFITE

Constituent	wt%	Range	SD	Probe standard
Na ₂ O	2.69	1.80–3.42	0.80	albite
MgO	4.76	4.04–5.57	0.65	syn. forsterite
Mn ₂ O ₃	1.79	1.58–1.94	0.15	syn. tephroite
Fe ₂ O ₃	37.36	36.54–38.12	0.56	syn. fayalite
P ₂ O ₅	34.68	34.33–35.09	0.33	fluorapatite
H ₂ O*	14.63			
Total	95.91			

* The amount of H₂O is based on results of the structure refinement.



FIG. 2. Phosphate nodules (dark masses) in place in the intermediate zone of the Angarf-Sud pegmatite. FOV is about 65 cm.



FIG. 3. Angarfite needles with bederite on etched triphylite; FOV 3 mm.

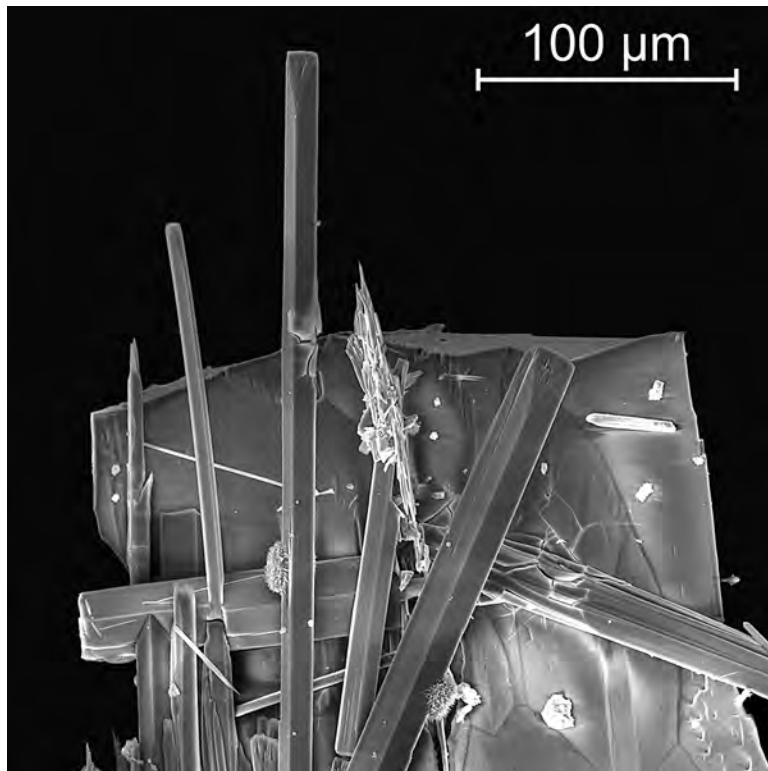


FIG. 4. SEM image of angarite needles on etched triphylite.

The details of the data collection and the final refinement of the structure are provided in Table 3. The final coordinates and displacement parameters of atoms are provided in Table 4. Selected interatomic distances are listed in Table 5, and bond valences, in Table 6. Tables of observed and calculated structure-factors are available from the Depository of Unpublished data on the Mineralogical Association of Canada website [document Angarite CM50_781].

ATOMIC ARRANGEMENT

The structure of angarite (Fig. 6) contains zig-zag chains of edge-sharing octahedra along c . The chains are linked into sheets parallel to $\{010\}$ by sharing corners with octahedra in adjacent chains and by sharing corners with peripheral PO_4 tetrahedra. Insular octahedra between the sheets share two sets of *cis* corners with tetrahedra in adjacent sheets, thereby linking the sheets into a framework. Channels parallel to c in the framework contain a partially occupied Na site and a disordered H_2O site. There remains additional residual electron density in the central region of the channel, which cannot be readily modeled as distinct atom-sites. This can readily account for the fact that the refined

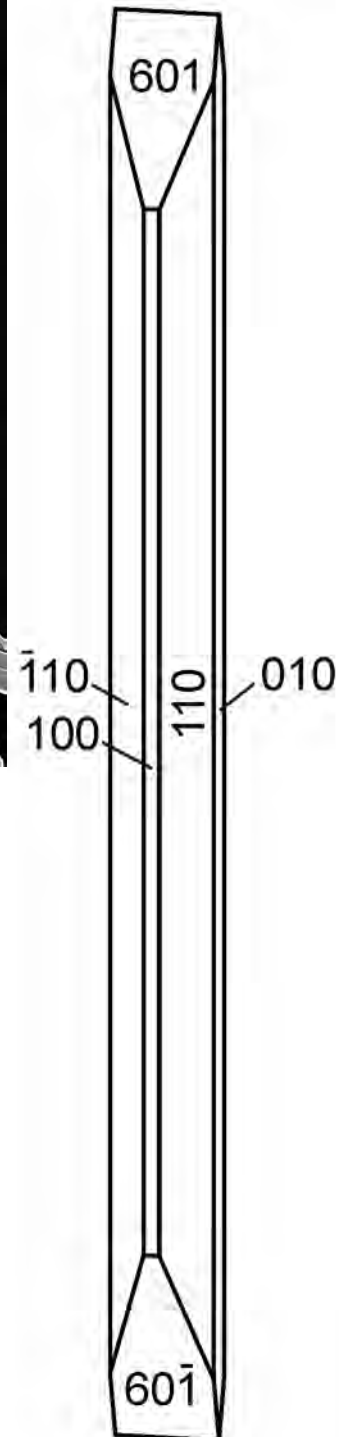


FIG. 5. Crystal drawing of angarite (clinographic projection in standard orientation).

TABLE 2. X-RAY POWDER-DIFFRACTION DATA FOR ANGARFITE

I_{obs}	d_{obs}	d_{calc}	I_{calc}	h	k	l	I_{obs}	d_{obs}	d_{calc}	I_{calc}	h	k	l
43	10.463(13)	10.4133	55	1	1	0	21	2.0798(14)	2.0827	6	5	5	0
100	9.016(5)	8.9541	100	0	2	0			2.0647	4	6	0	1
42	6.459(5)	6.4478	36	1	1	1			2.0528	5	0	0	4
3	5.052(10)	5.0478	3	2	0	1			1.9376	5	3	5	3
14	4.497(3)	4.4770	9	0	4	0	33	1.9259(4)	1.9272	5	4	6	2
		3.8195	5	1	1	2			1.9240	11	2	6	3
27	3.7311(11)	3.7320	16	0	2	2	15	1.8354(5)	1.8342	9	4	8	0
14	3.4751(14)	3.4711	10	3	3	0	15	1.7631(4)	1.7672	2	5	7	1
51	3.3550(5)	3.3494	45	2	4	1			1.7669	3	3	3	4
24	3.2034(7)	3.1999	6	4	0	0			1.7613	3	3	9	1
		3.1972	13	3	3	1	10	1.6724(9)	1.6747	2	4	8	2
29	3.0261(19)	3.0259	26	0	4	2			1.6726	6	2	8	3
7	2.926(8)	2.9188	4	3	1	2	10	1.6536(12)	1.6559	2	5	7	2
26	2.6518(15)	2.6507	15	3	3	2			1.6536	4	6	2	3
		2.6472	6	1	1	3	6	1.5957(11)	1.6119	3	4	4	4
24	2.6059(14)	2.6033	20	4	4	0			1.6000	2	8	0	0
18	2.5251(7)	2.5239	7	4	0	2			1.5907	2	2	0	5
		2.4292	4	4	2	2	14	1.5721(12)	1.5750	4	6	4	3
21	2.4235(4)	2.4227	8	2	2	3	25	1.4979(5)	1.5066	4	8	4	0
		2.4142	6	0	6	2			1.4989	8	2	4	5
3	2.343(3)	2.3527	2	5	3	0			1.4705	4	8	2	2
7	2.279(4)	2.2849	2	3	1	3	36	1.4626(2)	1.4657	7	6	6	3
2	2.1947(19)	2.1986	2	4	4	2			1.4605	5	4	10	2
		2.1938	2	2	4	3			1.4591	5	2	10	3

Note: d_{calc} and I_{calc} calculated from the crystal structure using JADE 9.1. The values of d_{obs} and d_{calc} are expressed in Å.

TABLE 3. ANGARFITE: DATA COLLECTION AND STRUCTURE-REFINEMENT DETAILS

Diffractometer	Rigaku R-Axis Rapid II
X-ray radiation, power	MoKα ($\lambda = 0.71075$ Å) / 50 kV, 40 mA
Temperature	298(2) K
Structural formula	$\text{Na}_{0.365}(\text{Fe}^{3+})_{0.797}\text{Mg}_{1.203}\text{Zn}(\text{PO}_4)_4(\text{OH})_4 \cdot 4\text{H}_2\text{O}$
Space group	C222 ₁
Unit-cell dimensions	a, b, c
a , b , c	12.7997(3), 17.9081(4), 8.2112(6) Å
Z	4
Volume	1882.16(15) Å ³
Density (for above formula)	2.7116 g/cm ³
Absorption coefficient	3.384 mm ⁻¹
$F(000)$	1524.7
Crystal size	320 × 140 × 50 mm
θ range	3.16 to 27.47°
Index ranges	$-16 \leq h \leq 16, -23 \leq k \leq 23, -10 \leq l \leq 10$
Reflections collected	10527
Reflections	2164 [$R_{\text{int}} = 0.0271$]
Reflections with $F_o > 4\sigma F$	2074
Completeness to $\theta = 27.48^\circ$	99.6%
Max., min. transmission	0.8490, 0.4106
Refinement method	Full-matrix least-squares on F^2
Parameters refined	175
GoF	1.056
Final R indices [$F_o > 4\sigma F$]	$R_1 = 0.0302$, $wR_2 = 0.0788$
R indices (all data)	$R_1 = 0.0316$, $wR_2 = 0.0799$
Largest diff. peak, hole	+0.925, -0.567 e Å ⁻³
Flack parameter	0.00(3)

Notes: $R_{\text{int}} = \sum |F_o^2 - F_c^2(\text{mean})| / \sum |F_o^2|$.

$\text{GoF} = S = \{\sum [w(F_o^2 - F_c^2)^2] / (n - p)\}^{1/2}$

$R_i = \sum |F_o| - |F_c| / \sum |F_o|$. $wR_2 = \{\sum [w(F_o^2 - F_c^2)^2] / \sum [w(F_o^2)^2]\}^{1/2}$; $w = 1/[\sigma^2(F_o^2) + (aP)^2 + bP]$, where a is 0.048, b is 5.918, and P is $[2F_c^2 + \text{Max}(F_o^2, 0)]/3$.

occupancy of the Na site provides considerably less Na than the chemical analysis, 0.365 vs 0.71 apfu.

The structure contains three distinct octahedral sites that contain Fe^{3+} , Mg^{2+} and Mn^{3+} , but all are dominantly occupied by Fe^{3+} . Neglecting the small amount of Mn^{3+} and refining the sites with joint occupancy considering only Fe^{3+} and Mg^{2+} , we infer that the insular site, Fe1, between the sheets contains $(\text{Fe}^{3+})_{0.96}\text{Mg}^{2+}_{0.04}$, and the two sheet sites, Fe2 and Fe3, contain $(\text{Fe}^{3+})_{0.66}\text{Mg}^{2+}_{0.34}$ and $(\text{Fe}^{3+})_{0.76}\text{Mg}^{2+}_{0.24}$, respectively. The calculated bond-valence sums for the Fe2 and Fe3 sites (Table 6), 2.644 and 2.693 vu, respectively, fit well with the theoretical values based upon the mixed-valence occupancies, 2.68 and 2.76 vu.

Except for very minor deviations in geometry, the sheet of octahedra and tetrahedra in the structure of angarfite (Fig. 7) is identical to those in the structures of bakhchisaraitsevite, $\text{Na}_2\text{Mg}_5(\text{PO}_4)_4 \cdot 7\text{H}_2\text{O}$ (Liferovich *et al.* 2000, Yakubovich *et al.* 2000), and mejillonesite, $\text{NaMg}_2(\text{PO}_3\text{OH})(\text{PO}_4)(\text{OH}) \cdot \text{H}_5\text{O}_2$ (Atencio *et al.* 2012). The cell parameters (Table 7) corresponding to the sheet dimensions are comparable: a and c for angarfite, b and a for bakhchisaraitsevite and b and c for mejillonesite. The structures are also similar in that they contain Na atoms and H_2O in the interlayer region; however, the structures differ significantly in the linkages between the sheets. As noted above, insular octahedra in the angarfite structure link the sheets via bonds to tetra-

TABLE 4. FINAL COORDINATES AND DISPLACEMENT PARAMETERS (\AA^2) OF ATOMS IN ANGARFITE

	x/a	y/b	z/c	U_{eq}	U_{11}	U_{22}	U_{33}	U_{23}	U_{13}	U_{12}
Fe1*	0.11879(4)	0.0000	0.0000	0.0090(2)	0.0089(3)	0.0080(3)	0.0100(3)	0.0002(2)	0.000	0.000
Fe2*	0.13261(6)	0.74543(3)	0.81131(8)	0.0108(3)	0.0114(4)	0.0122(4)	0.0089(4)	0.00018(19)	0.0011(2)	0.0035(3)
Fe3*	0.12964(5)	0.75536(3)	0.20026(7)	0.0124(2)	0.0107(4)	0.0161(4)	0.0105(3)	0.00245(19)	-0.0004(2)	0.0024(3)
P1	0.96324(6)	0.84964(4)	0.98805(13)	0.0103(2)	0.0097(3)	0.0092(3)	0.0119(4)	-0.0011(3)	0.0006(4)	-0.0012(3)
P2	0.29583(6)	0.14343(4)	0.00075(14)	0.01082(19)	0.0109(3)	0.0108(4)	0.0109(4)	-0.0003(4)	0.0003(4)	-0.0016(3)
Na*	0.4776(10)	0.0000	0.0000	0.089(5)	0.114(10)	0.017(4)	0.135(11)	0.012(6)	0.000	0.000
O1	0.8939(2)	0.82487(14)	0.8488(3)	0.0175(6)	0.0162(14)	0.0172(12)	0.0189(12)	-0.0035(9)	-0.0053(12)	0.0008(10)
O2	0.9975(2)	0.93072(13)	0.9619(3)	0.0148(5)	0.0132(10)	0.0091(10)	0.0220(14)	0.0001(9)	-0.0010(9)	-0.0014(9)
O3	0.9034(2)	0.84281(15)	0.1503(3)	0.0175(6)	0.0170(14)	0.0188(12)	0.0169(12)	-0.0016(10)	0.0041(11)	0.0004(11)
O4	0.06196(16)	0.79926(12)	0.9985(4)	0.0133(4)	0.0125(9)	0.0139(10)	0.0136(10)	0.0006(11)	-0.0001(12)	0.0034(8)
O5	0.22146(19)	0.07858(14)	0.0180(4)	0.0190(5)	0.0213(11)	0.0139(11)	0.0217(13)	0.0008(12)	0.0026(12)	-0.0061(9)
O6	0.40855(18)	0.11783(15)	0.9994(4)	0.0242(5)	0.0155(11)	0.0289(13)	0.0281(13)	0.0000(14)	-0.0005(17)	0.0048(10)
O7	0.2777(2)	0.19970(15)	0.1426(3)	0.0141(6)	0.0153(14)	0.0145(12)	0.0124(12)	-0.0016(10)	-0.0010(10)	-0.0025(10)
O8	0.2712(2)	0.18688(15)	0.8404(3)	0.0148(6)	0.0166(14)	0.0156(12)	0.0121(12)	0.0014(10)	0.0022(10)	-0.0010(11)
OH1	0.0000	0.6997(2)	0.2500	0.0168(8)	0.016(2)	0.0150(18)	0.0196(19)	0.000	0.0041(16)	0.000
H1	-0.007(9)	0.658(3)	0.186(9)	0.020						
OH2	0.0000	0.6900(2)	0.7500	0.0201(9)	0.018(2)	0.0205(19)	0.021(2)	0.000	-0.0011(17)	0.000
H2	-0.036(7)	0.676(5)	0.840(8)	0.024						
OH3	0.1702(2)	0.68182(14)	0.0128(4)	0.0225(6)	0.0290(13)	0.0198(12)	0.0187(13)	-0.0025(12)	0.0012(14)	-0.0009(10)
H3	0.237(2)	0.669(2)	0.002(8)	0.027						
OW1	0.1272(2)	0.98473(13)	0.2488(3)	0.0180(5)	0.0238(12)	0.0158(12)	0.0144(12)	0.0032(10)	0.0040(10)	0.0018(11)
HW1A	0.102(3)	1.0160(17)	0.315(5)	0.022						
HW1B	0.112(4)	0.9381(14)	0.268(6)	0.022						
OW2A*	0.6548(13)	0.0335(8)	0.136(2)	0.092(7)						
OW2B*	0.604(2)	0.0076(14)	0.214(3)	0.177(11)						

* Site occupancies: Fe1: Fe, Mg 0.961, 0.039(8), Fe2: Fe, Mg 0.656, 0.344(7), Fe3: Fe, Mg 0.762, 0.238(7); Na 0.365(14); OW2A: 0.50(3); OW2B: 0.50(3).

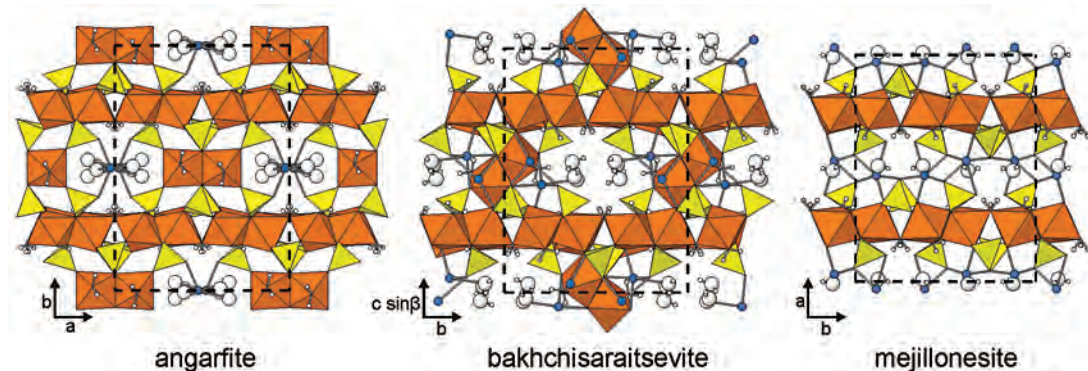


FIG. 6. Structures of angarafite, bakhchisaraitsevite and mejillonesite. The PO_4 tetrahedra are yellow. All octahedra are shown in orange. The octahedrally coordinated cations are Fe^{3+} in angarafite, Mg^{2+} in bakhchisaraitsevite and mejillonesite. Sodium atoms are shown as blue spheres, isolated O atoms as large white spheres, and H atoms as small white spheres.

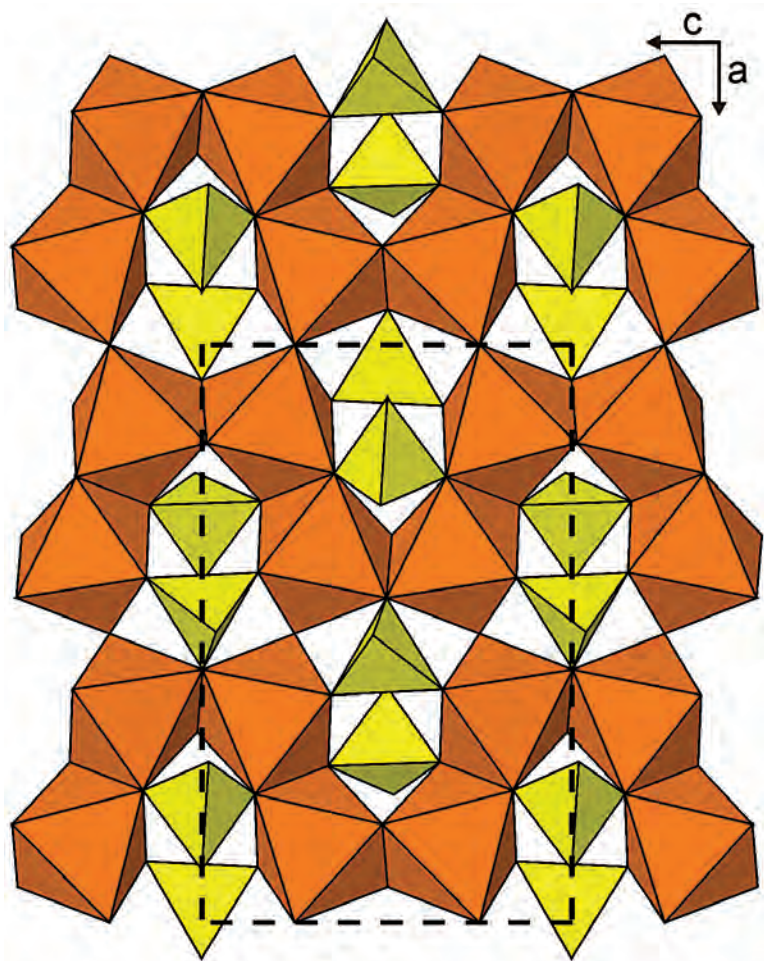


FIG. 7. Sheet of octahedra and tetrahedra in the angarfite structure. Except for minor geometric deviations, this sheet is identical to those in bakhchisaraitsevite and mejillonesite. The PO_4 tetrahedra are shown in yellow, and the Fe^{3+}O_6 octahedra are orange.

hedra in the sheets. In the bakhchisaraitsevite structure, $[\text{Mg}_2\text{O}_{10}]$ dimers of edge-sharing octahedra link the sheets via bonds to both octahedra and tetrahedra in the sheets. The sheets are most loosely linked in the structure of mejillonesite. In this case, there is no inter-sheet bonding between octahedra and tetrahedra. The only linkage is via Na–O bonds and hydrogen bonding.

Mélonjosephite, for which Angarf-Sud is also the type locality (Fransolet 1973), also has a framework structure consisting of FeO_6 octahedra and PO_4 tetrahedra, and its framework also contains channels hosting a large cation (Ca) (Kampf & Moore 1977). However, the structures of angarfite and mélonjosephite are not closely related.

TABLE 5. SELECTED BOND-DISTANCES (Å) AND ANGLES (°) FOR ANGARFITE

Fe1–O5 (×2)	1.931(2)	Fe2–O1	1.966(3)	Fe3–OH1	1.978(2)	
Fe1–O2 (×2)	2.012(2)	Fe2–O4	2.027(3)	Fe3–O7	2.016(3)	
Fe1–OW1 (×2)	2.064(3)	Fe2–OH2	2.030(2)	Fe3–O4	2.028(3)	
<Fe–O>	2.002	Fe2–O8	2.042(3)	Fe3–O3	2.034(3)	
		Fe2–OH3	2.065(3)	Fe3–OH3	2.091(3)	
		Fe2–O7	2.135(3)	Fe3–O8	2.113(3)	
		<Fe–O>	2.044	<Fe–O>	2.044	
Na–O6 (×2)	2.287(6)	P1–O1	1.514(3)	P2–O5	1.508(2)	
Na–OW2B (×2)	2.388(23)	P1–O2	1.532(2)	P2–O6	1.514(2)	
Na–OW2B (×2)	2.574(32)	P1–O3	1.541(3)	P2–O7	1.558(3)	
Na–OW2A (×2)	2.598(19)	P1–O4	1.555(2)	P2–O8	1.561(3)	
<Na–O>	2.46	<P–O>	1.536	<P–O>	1.535	
Hydrogen bonds (D: donor, A: acceptor)						
D–H	d(D–H)	d(H–A)	<DHA	d(D–A)	A	<HDH
OH1–H1	0.91(3)	2.01(7)	141(8)	2.784(4)	O6	
OH2–H2	0.91(3)	1.81(4)	162(9)	2.690(4)	O6	
OH3–H3	0.89(3)	2.35(5)	139(5)	3.083(4)	O1	
OW1–HW1A	0.85(2)	2.00(3)	162(4)	2.811(3)	O2	116
OW1–HW1B	0.87(2)	1.84(3)	167(5)	2.702(4)	O3	

TABLE 6. BOND-VALENCE SUMMATIONS FOR ANGARFITE

	O1	O2	O3	O4	O5	O6	O7	O8	OH1	OH2	OH3	OW1	OW2A	OW2B	Σ
Fe1		0.501 × 2→			0.624 × 2→							0.436 × 2→			3.122
Fe2	0.539			0.457			0.342	0.439		0.454 × 2↓	0.413				2.644
Fe3			0.457	0.465			0.480	0.369	0.530 × 2↓		0.392				2.693
P1	1.321	1.258	1.228	1.182											4.989
P2					1.343	1.321	1.173	1.163							5.000
Na						0.267						0.058	0.102 0.062		0.979
H1						0.120			0.880						1.000
H2						0.180				0.820					1.000
H3	0.070										0.930				1.000
HW1A		0.130										0.870			1.000
HW1B			0.170									0.830			1.000
Σ	1.930	1.889	1.855	2.104	1.967	1.888	1.995	1.971	1.940	1.728	1.735	2.136	0.058	0.164	

Notes: Multiplicity is indicated by $\times \rightarrow l$; bond strengths are taken from Brown & Altermatt (1985). Bond strengths for the Fe1, Fe2 and Fe3 sites are based upon the refined site-occupancies. Hydrogen-bond strengths are based on H–O bond lengths, also from Brown & Altermatt (1985). The hydrogen-bond contributions from OW2A and OW2B are not included. Values are quoted in valence units ($v.u$).

TABLE 7. COMPARISON OF SPACE GROUPS AND UNIT-CELL PARAMETERS OF ANGARFITE, BAKHCHISARAITSEVITE AND MEJILLONESITE

Mineral	angarite	bakhchisaraitsevite	mejillonesite
Space group	C222,	P2 ₁ /c	Pbc _a
<i>a</i> (Å)	12.7997(3)	8.3086(8)	16.295(1)
<i>b</i> (Å)	17.9081(4)	12.906(1)	13.009(2)
<i>c</i> (Å)	8.2112(6)	17.486(2)	8.434(1)
β (°)		102.01(1)	

ACKNOWLEDGEMENTS

The manuscript benefitted from comments by reviewers Frédéric Hatert and Kim Tait. We also acknowledge the very able shepherding of the manuscript by Associate Editor Miguel Galliski and the astute editing of Editor-in-Chief Robert F. Martin. The EMP analyses were supported by a grant to Caltech from the Northern California Mineralogical Association. The remainder of this study was funded by the John Jago Trelawney Endowment to the Mineral Sciences Department of the Natural History Museum of Los Angeles County. Finally, we wish to pay special tribute to Petr Černý for ground-breaking contributions to the understanding of pegmatites.

REFERENCES

- ARMSTRONG, J.T. (1995): CITZAF—a package of correction programs for the quantitative electron microbeam X-ray analysis of thick polished materials, thin-films and particles. *Microbeam Anal.* **4**, 177-200.
- ATENCIO, D., CHUKANOV, N.V., NESTOLA, F., WITZKE, T., COUTINHO, J.M.V., ZADOV, A.E., CONTRERA FILHO, R.R. & FÄRBER, G. (2012): Mejillonesite, a new acid sodium, magnesium hydrogen phosphate mineral from Mejillones, Antofagasta, Chile. *Am. Mineral.* **97**, 19-25.
- BROWN, I.D. & ALTERMATT, D. (1985): Bond-valence parameters obtained from a systematic analysis of the inorganic crystal structure database. *Acta Crystallogr.* **B41**, 244-247.
- BURLA, M.C., CALIANDRO, R., CAMALLI, M., CARROZZINI, B., CASCARANO, G.L., DE CARO, L., GIACOVAZZO, C., POLIDORI, G. & SPAGNA, R. (2005): SIR2004: an improved tool for crystal structure determination and refinement. *J. Appl. Crystallogr.* **38**, 381-388.
- FRANSOLET, A.-M. (1973): La mélionjosephite, CaFe²⁺Fe³⁺(PO₄)₂(OH), une nouvelle espèce minérale. *Bull. Minéral.* **96**, 135-142.
- FRANSOLET, A.-M. (1975): On scorzalite from the Angarf-Sud pegmatite, Zenaga Plain, Anti-Atlas, Morocco. *Fortschr. Mineral.* **52**, 285-291.
- FRANSOLET, A.-M. (1987): Les phosphates secondaires de la pegmatite d'Angarf-Sud, Plaine des Zenaga, Anti-Atlas, Maroc. *Notes et Mémoires du Service Géologique du Maroc* **43**(321), 339-347.
- FRANSOLET, A.-M., ABRAHAM, K. & SPEETJENS, J.-M. (1985): Evolution génétique et signification des associations de phosphates de la pegmatite d'Angarf-Sud, Plaine de Tazenakht, Anti-Atlas, Maroc. *Bull. Minéral.* **108**, 551-574.
- GALLISKI, M.A., COOPER, M.A., HAWTHORNE, F.C. & ČERNÝ, P. (1999): Bederite, a new pegmatite mineral from Nevados de Palermo, Argentina: description and crystal structure. *Am. Mineral.* **84**, 1674-1679.
- JOURAVSKY, G. & DESTOMBES, J. (1961): Les différents types de minéralisations de l'Anti-Atlas. Leur cadre géologique et les méthodes de leur prospection. *Mines et Géologie* **13**, 19-57.
- KAMPF, A.R. & MOORE, P.B. (1977): Mélonjosephite, calcium iron hydroxy phosphate: its crystal structure. *Am. Mineral.* **62**, 60-66.
- KAMPF, A. R., STEELE, I. M. & LOOMIS, T. (2008): Jahnsite-(NaFeMg), a new mineral from the Tip Top mine, Custer County, South Dakota: description and crystal structure. *Am. Mineral.* **93**, 940-945.
- LIFEROVICH, R.P., PAKHOMOVSKY, Y.A.A., YAKUBOVICH, O.V., MASSA, W., LAAJOKI, K., GEHÖR, S., BOGDANOVA, A.N. & SOROKHTINA, N.V. (2000): Bakhchisaraitsevite, Na₂Mg₅[PO₄]₄•7H₂O, a new mineral from hydrothermal assemblages related to phoscorite–carbonatite complex of the Kovdor massif, Russia. *Neues Jahrb. Mineral., Monatsh.*, 402-418.
- MANDARINO, J.A. (1981): The Gladstone–Dale relationship. IV. The compatibility concept and its application. *Can. Mineral.* **19**, 441-450.
- SHELDICK, G.M. (2008): A short history of SHELX. *Acta Crystallogr.* **A64**, 112-122.
- THOMAS, R.J., CHEVALLIER, L.P., GREESE, P.G., HARMER, R.E., EGLINGTON, B.M., ARMSTRONG, R.A., DE BEER, C.H., MARTINI, J.E.J., DE KOCK, G.S., MACEY, P.H. & INGRAM, B.A. (2002): Precambrian evolution of the Sirwa Window, Anti-Atlas Orogen, Morocco. *Precamb. Res.* **118**, 1-57.
- YAKUBOVICH, O.V., MASSA, W., LIFEROVICH, R.P. & PAKHOMOVSKY, Y.A. (2000): The crystal structure of bakhchisaraitsevite, [Na₂(H₂O)₂]•{[Mg_{4.5}Fe_{0.5}](PO₄)₄(H₂O)₅}, a new mineral species of hydrothermal origin from the Kovdor phoscorite–carbonatite complex, Russia. *Can. Mineral.* **38**, 831-838.